Tertiary treatment of urban wastewater by solar and UV-C driven advanced oxidation with peracetic acid: effect on contaminants of emerging concern and antibiotic resistance

Elsevier Editorial System(tm) for Water Research

Manuscript Draft

Manuscript Number:

Title: Tertiary treatment of urban wastewater by solar and UV-C driven advanced oxidation with peracetic acid: effect on contaminants of emerging concern and antibiotic resistance

Article Type: Research Paper

Keywords: advanced oxidation processes; antibiotic resistant bacteria; peracetic acid; solar driven processes; wastewater treatment; water disinfection

Corresponding Author: Professor Luigi Rizzo, PhD

Corresponding Author's Institution: University of Salerno

First Author: Luigi Rizzo, PhD

Order of Authors: Luigi Rizzo, PhD; Teresa Agovino; Samira Nahim Granados; Maria Castro-Alférez; Pilar Fernández-Ibáñez; Maria I Polo-López

Abstract: Photo driven advanced oxidation process (AOP) with peracetic acid (PAA) has been poorly investigated in water and wastewater treatment so far. In the present work its possible use as tertiary treatment of urban wastewater to effectively minimize the release into the environment of contaminants of emerging concern (CECs) and antibiotic resistant bacteria was investigated. Different initial PAA concentrations, two light sources (sunlight and UV-C) and two different water matrices (groundwater (GW) and wastewater (WW)) were studied. Low PAA doses were found to be effective in the inactivation of antibiotic resistant Escherichia coli (AR E. coli) in GW, being UV-C driven process faster (detection limit (DL) achieved for a cumulative energy (QUV) of 0.3 kJL-1 with 0.2 mg PAA L-1) than solar driven one (DL achieved at QUV=4.4 kJL-1 with 0.2 mg PAA L-1). Really fast inactivation rates of indigenous AR E. coli were observed in WW. Higher QUV and PAA initial doses were necessary to effectively remove the three target CECs (carbamazepine (CBZ), diclofenac and sulfamethoxazole), being CBZ the more refractory one. In conclusion, photo driven AOP with PAA can be effectively used as tertiary treatment of urban wastewater but initial PAA dose should be optimized to find the best compromise between target bacteria inactivation and CECs removal as well as to prevent scavenging effect of PAA on hydroxyl radicals because of high PAA concentration.

Suggested Reviewers: Monica Brienza
Montpellier University
monica.brienza@ird.fr

Manuel A Manzano Quiñones
University of Cadiz
manuel.manzano@uca.es

Popi Karaolia

University of Cyprus
Pkarao01@ucy.ac.cy

Sureyya Meric
Namik Kemal University
smeric@nku.edu.tr

Dear Editor,

we kindly ask you to consider for possible publication in "Water Research" journal our research paper entitled:

Tertiary treatment of urban wastewater by solar and UV-C driven advanced oxidation with peracetic acid: effect on contaminants of emerging concern and antibiotic resistance

Photo driven advanced oxidation process (AOP) with peracetic acid (PAA) has been poorly investigated in water and wastewater treatment so far. In the present work, its possible use as tertiary treatment of urban wastewater to effectively minimize the release into the environment of contaminants of emerging concern (CECs) and antibiotic resistant bacteria was investigated. In particular, the effect of two light sources (sunlight and UV-C) on the simultaneous inactivation of antibiotic resistant *E. coli* and removal from real wastewater of three CECs (namely, carbamazepine, diclofenac and sulfamethoxazole) (spiked) at quite realistic concentrations was investigated. To our knowledge, this is the first work where sunlight/PAA process has been investigated. In our opinion the results achieved can significantly advance the knowledge about photo driven AOP with PAA and its contribution to successfully address emerging challenges in urban wastewater treatment.

Our manuscript perfectly fits the scopes of your prestigious journal, and we trust you will find of interest for you and journal readers our work.

This work has not been published previously - also not in any other language-, it is not under consideration for publication elsewhere, and if accepted it will not be published elsewhere in the same form, or in any other language, without the written consent of the publisher.

Best regards

The corresponding authors

Luigi Rizzo

María Inmaculada Polo-López

Highlights

- First time sunlight/PAA investigated in the removal of CECs
- Low PAA doses effective in the inactivation of AR *E. coli* by UV-C/PAA and sunlight/PAA
- Higher Q_{UV} and PAA initial doses are necessary to effectively remove the target CECs
- UV-C/PAA faster than sunlight/PAA in AR *E. coli* inactivation and CECs removal
- Sunlight/PAA possible option for tertiary treatment in small wastewater treatment plants

Graphical Abstract

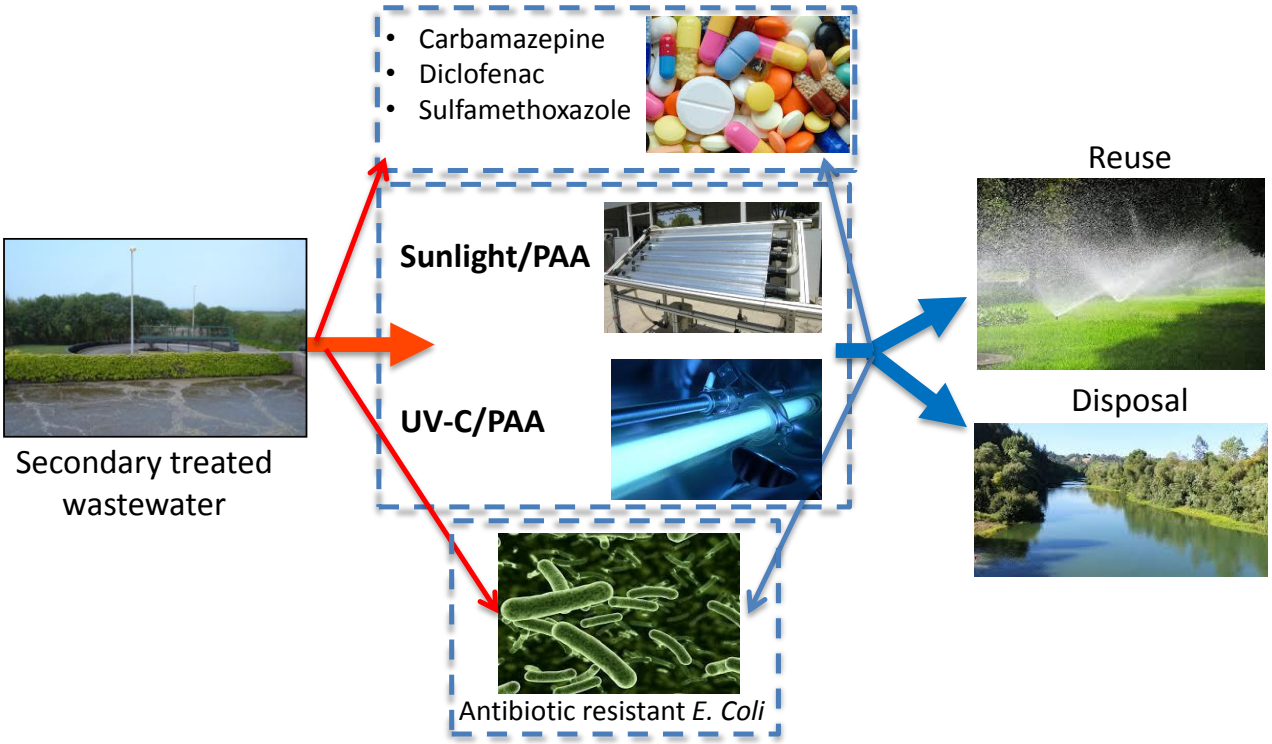

Tertiary treatment of urban wastewater by solar and UV-C driven advanced oxidation with peracetic acid: effect on contaminants of emerging concern and antibiotic resistance

Luigi Rizzo[1,*], Teresa Agovino[1], Samira Nahim-Granados [2], María Castro-Alférez [2], Pilar Fernández-Ibáñez [3], María Inmaculada Polo-López[2,*]

[1]Department of Civil Engineering, University of Salerno, Via Giovanni Paolo II 132, 84084 Fisciano (SA), Italy

[2] CIEMAT-Plataforma Solar de Almeria, P.O. Box 22, Tabernas (Almería), Spain.

[3]Nanotechnology and Integrated BioEngineering Centre, School of Engineering, University of Ulster, Newtownabbey, Northern Ireland, United Kingdom

*Corresponding authors: l.rizzo@unisa.it, mpolo@psa.es

Abstract

Photo driven advanced oxidation process (AOP) with peracetic acid (PAA) has been poorly investigated in water and wastewater treatment so far. In the present work its possible use as tertiary treatment of urban wastewater to effectively minimize the release into the environment of contaminants of emerging concern (CECs) and antibiotic resistant bacteria was investigated. Different initial PAA concentrations, two light sources (sunlight and UV-C) and two different water matrices (groundwater (GW) and wastewater (WW)) were studied. Low PAA doses were found to be effective in the inactivation of antibiotic resistant *Escherichia coli* (AR *E. coli*) in GW, being UV-C driven process faster (detection limit (DL) achieved for a cumulative energy (Q_{UV}) of 0.3 kJL^{-1} with 0.2 mg PAA L^{-1}) than solar driven one (DL achieved at Q_{UV}=4.4 kJL^{-1} with 0.2 mg PAA L^{-1}). Really fast inactivation rates of indigenous AR *E. coli* were observed in WW. Higher Q_{UV} and PAA initial doses were necessary to effectively remove the three target CECs (carbamazepine (CBZ), diclofenac and sulfamethoxazole), being CBZ the more refractory one. In conclusion, photo driven AOP with PAA can be effectively used as tertiary treatment of urban wastewater but initial PAA dose should be optimized to find the best compromise between target bacteria inactivation and CECs removal as well as to prevent scavenging effect of PAA on hydroxyl radicals because of high PAA concentration.

Keywords: advanced oxidation processes, antibiotic resistant bacteria, peracetic acid, solar driven processes, wastewater treatment, water disinfection.

1. Introduction

The concern for the release into the environment of micro-contaminants from point sources, such as wastewater treatment plants (Petrie et al., 2015), as well as the need of wastewater reuse, due to the lack of fresh water sources (Fatta Kassinos, 2015), have been stimulating the discussion in the last years about new relevant regulations (JRC, 2015; Brack et al., 2017) to make urban wastewater treatment plants (UWTPs) effluents safer. As matter of fact, because of inconsistent national legislation across Member States, the European Commission is working to a legislative proposal on minimum quality requirements (MQR) for water reuse in agricultural irrigation and aquifer recharge (Rizzo et al., 2018). Meanwhile, in the attempt to minimize the release of micro-contaminants (also known as contaminants of emerging concern, CECs) from UWTPs in the environment, Switzerland enacted a regulation entered into force on January 2016, which requires the upgrade of UWTPs within the next twenty years (www.bafu.admin.ch). Accordingly, a selection of CECs from a list of twelve compounds need to be removed by 80% (Bourgin et al. 2018). The increasing interest toward CECs and other emerging contaminants, such as antibiotic resistant bacteria (ARB) and genes (ARGs), as well as the ongoing discussion on new related regulations, are driven the attention on UWTPs that are not or poorly effective to successfully address these new challenges (Rizzo et al., 2013; Petrie et al., 2015; Krzeminski et al., 2019). In a multi-barrier approach, typically implemented in UWTPs trains, the most important role to minimize the release of CECs and the risk of antibiotic resistance spread into the environment relies on tertiary treatment (Ferro et al., 2015; Bourgin et al. 2018). Unfortunately, consolidated tertiary treatments either did not show to be effective or did result in some drawbacks. As matter of fact, chlorination, typically used as disinfection step before UWTP effluent disposal or reuse, is poorly effective in the removal of CECs (Fu et al., 2018) and in controlling antibiotic resistance (Fiorentino et al., 2015; Yuan et al., 2015), as well as results in the formation of

hazardous disinfection by-products (DBPs) (Huang et al., 2016; Keun-Young et al., 2016). UV-C disinfection is effective in the inactivation of pathogens when sand filtration is used as pre-treatment, but poor or not effective at all (depending on the characteristics of the target molecule) in the removal of CECs (Lian et al., 2015). Tertiary treatment by ozonation can inactivate pathogens and remove CECs, but an additional post-treatment step can be necessary to remove ozonation by products (i.e., nitrosodimetylamine and bromate) (Hollender et al., 2009). Activated carbon adsorption is also an effective tertiary treatment for the removal of CECs (Rizzo et al., 2015; Ahmed, 2017) but an additional disinfection process may be necessary, in particular to meet more stringent standards for wastewater reuse. Due to their efficiency in the removal of CECs and inactivation of pathogens because of the formation of reactive oxygen species (ROS), such as hydroxyl radicals ($HO^{\bullet}$), advanced oxidation processes (AOPs) represent a possible alternative to conventional tertiary treatments. AOPs can be classified in different ways, one being photo (among which UV/H_2O_2, photo-Fenton and TiO_2 photocatalysis) and not photo (such as Fenton, O_3, O_3/H_2O_2 etc.) driven AOPs. Photo driven AOPs, can be also operated with solar radiation to save energy costs (Malato et al., 2009). Homogeneous photo driven AOPs (such as UV/H_2O_2 and photo-Fenton) are more attractive than heterogeneous photocatalytic processes (such as UV/TiO_2) for short term application as tertiary treatment method of urban wastewater. As matter of fact, the technology of heterogeneous processes is not yet fully mature for large scale applications, basically for limitations related either to catalyst removal after treatment or fixing catalyst on a support (Sacco et al., 2018), and it would be more expensive than homogeneous photo driven AOPs based technology. Peracetic acid (PAA) is increasingly used as alternative option to chlorination in wastewater disinfection (Antonelli et al., 2013; Formisano et al., 2016). However, disinfection efficiency (Formisano et al., 2016) and CECs removal (Cai et al., 2017) may be improved by coupling PAA with UV radiation, due to the formation of $HO^{\bullet}$.

Accordingly, it is worthy of investigation possible use of this process as homogeneous photo driven AOP for tertiary treatment of urban wastewater. In particular, before possible upscale it would be of interest to learn process efficiency in the removal of CECs at environmentally significant concentrations as well as its effect on antibiotic resistance. Accordingly, in the present work, UV/PAA process at pilot scale was investigated for the first time in the inactivation of an antibiotic resistant (AR) (sulfamethoxazole) *Escherichia coli* (*E. coli*) strain, and in the degradation of a mixture of three CECs: (anticonvulsant) Carbamazepine (CBZ), (analgesic) Diclofenac (DCF) and (antibiotic) Sulfamethoxazole (SMX), at initial concentration of 100 μgL^{-1} each, in a lower complexity aqueous matrix (namely groundwater (GW)). Subsequently, UV/PAA process was investigated in wastewater (WW) treatment for the inactivation of indigenous AR *E. coli* and the degradation of the same mixture of CECs. The effect of light source (solar light Vs UV-C radiation) was also investigated in both aqueous matrices (GW and WW). *E. coli* was chosen as model microorganism because it is considered among the most important vectors in the dissemination of antimicrobial resistance in the environment (Rizzo et al., 2013) as well as because it is used as pathogen indicator in regulations and guide lines for wastewater disposal and reuse (USEPA, 2012; ISO, 2015). CBZ, DCF and SMX were selected as model CECs because typically detected in urban wastewater (Petrie et al., 2015).

2. Material and methods

2.1 Chemicals

Carbamazepine (CBZ), Diclofenac (DCF) and Sulfamethoxazole (SMX), all high purity grade (>99%), were purchased from Sigma-Aldrich. Peracetic Acid (PAA) solution, containing 30% w/w of PAA and 4.5 % w/w of H_2O_2 was purchased from Sigma-Aldrich

and used as obtained. Sodium thiosulfate ($Na_2S_2O_3$, 99% w/w) and bovin liver catalase were used, as received from Sigma-Aldrich. Titanium IV oxysulfate (Riedel-de-Haën, Germany) was used, as obtained from the manufacturer.

2.2 Water matrices

To evaluate water matrix effect on UV/PAA process tests were performed with both GW and wastewater WW. GW was collected from a borehole located on the PSA site with depth of approximately 200 m. Physical-chemical characteristics of both water matrices are given in Table 1.

Table 1

GW samples were inoculated with SMX resistant *E. coli* strain selected from the effluent of the biological process (activated sludge) of Almeria (Spain) UWTP, according to the procedure explained in the subsequent paragraph 2.4. WW samples were taken from the same UWTP during spring-summer time (June-August 2017), at the same location and used for disinfection/oxidation experiments without inoculum. Samples were collected in amber glass bottles and stored at 4 °C for a maximum of two days.

2.3 AOPs and control experiments

Experimental design included two pilot scale reactors namely a Compound Parabolic Collector (CPC) for outdoor sunlight experiments and UV-C reactor (UVC).

138

139 2.3.1 Sunlight/PAA experiments with CPC

140 The CPC reactor used was previously described (Polo-López et al., 2010). Briefly, it
141 consists of two 60 L tube modules, each one equipped with 10 cylindrical glass tubes made
142 of borosilicate glass, with a diameter of 5 cm, a length of 150 cm and a thickness of 2.5
143 mm, to allow a 90% transmission of UVA in the natural solar spectrum. The photoreactor
144 is titled at 37° with respect to the horizontal to maximize solar radiation. A tank housed in
145 the lower part of the pilot plant is connected to a pump, which allowed to operate the
146 modules in a recirculation mode. The CPC reactor has a total illuminated volume of 45 L
147 and it was operated with a water flow rate of 30 $Lmin^{-1}$. This flow rate guarantees a
148 turbulent regime, which results in a proper homogenization of water samples and in a good
149 contact between bacteria, contaminants and oxidant. Disinfection experiments were carried
150 out during 300 minutes of solar exposure on clear sunny days at PSA from May 2017 to
151 August 2017. More specifically, firstly the solar photoreactor was filled in with 60 L of
152 water matrix (GW or RW) and then, the mixture of the three CECs (100 μgL^{-1} of initial
153 concentration each) and the sulfamethoxazole resistant *E.coli* solution (10^6 CFU mL^{-1}
154 initial bacterial density) were spiked in. After 5 minute of homogenization with the CPC
155 still covered, control sample was taken in order to ensure the presence of bacteria and
156 contaminants. Then, PAA was added to the reactor tank and after 10 minute of
157 recirculation, the experiment started as the cover was removed. Samples were collected at
158 regular intervals depending on the treatment. Water temperature ranged from 21.0 to 47.7
159 °C and pH ranged from 8.04 to 9.41. A fixed pyranometer (Model CUV5, 280-400 nm,
160 Kipp & Zonen, Netherlands) registered in continuous the incident light. The inactivation
161 and degradation rates were plotted as a function of both the experimental time (t) and the
162 cumulative energy per unit of volume (Q_{UV}) received in the photoreactor, commonly used

163 to compare results under different condition (Malato et al., 2009), and calculated by
164 Equation (1):

165 $$Q_{UV,n} = Q_{UV,n-1} + \Delta t_n \cdot UV_{G,n} \cdot A_r/V_t \qquad \Delta t_n = t_n - t_{n-1} \qquad \text{(Eq.1)}$$

166 where $Q_{UV,n}$ and $Q_{UV,n-1}$ is the UV energy accumulated per liter (kJ L^{-1}) at times n and n-1,
167 $UV_{G,n}$ is the average incident radiation on the irradiated area, Δt_n is the experimental time
168 of sample, A_r is the illuminated area of the reactor (m^2) and V_t is the total volume of water
169 treated (L). Each experiment was performed in duplicate, between 10 am to 16 pm local
170 time, and the results were plotted as the average of the two replicates.

171

172 2.3.2 UVC plant

173 The UVC reactor is a plant equipped with three UVC lamps (254 nm peak wavelengths,
174 230 W) connected in series, with a flexible configuration that allow the system to operate
175 with a single lamp, two or three lamps in recirculating batch mode or continuous flow
176 mode. In this study, only one lamp was used and the illuminated volume was 4.17 L, which
177 corresponds to a total volume in the plant of 80 L. Disinfection/oxidation experiments were
178 carried out during 180 minutes at PSA from May 2017 to August 2017. More specifically,
179 firstly the reactor was filled in with water matrix (GW or WW) and then, the mixture of the
180 three CECs (100 μgL^{-1}) and the sulfamethoxazole resistant *E.coli* solution (10^6 $CFUmL^{-1}$)
181 were spiked in. After 15 minute of homogenization, with the lamp still switched off, initial
182 sample was taken in order to ensure the presence of bacteria and contaminants. Then, PAA
183 was added to the reactor tank and after 15 minute of recirculation, the experiment started
184 and the lamp was switched on. Samples were collected at regular intervals depending on
185 the treatment. A fixed controller (ProMinent) housed in the back of the reactor, monitored
186 in continuous water flow rate (46 $Lmin^{-1}$) and UVC lamp intensity (33.7 Wm^{-2} for WW

187 and 99.7 Wm^{-2} for GW). The equipment registers, in continuous during the test, the sensor
188 measurements in terms of incident irradiation (Wm^{-2}), which is the UVC radiation energy
189 rate incident on a surface per unit area. The accumulated energy was calculated according
190 to Eq. 2:

191 $$Q_{UVC}\ (kJ\ L^{-1}) = \text{Dose}\ (Jm^{-2}) \cdot A_i/V_T (m^2 L^{-1})(kJ(1000\ J)^{-1}) \quad \text{(Eq.2)}$$

192 where Q_{UVC} is the accumulated UVC energy per L, Dose is the UVC ultraviolet irradiation
193 (Wm^{-2}) emitted by the lamp multiplied by the illumination time, A_i (0.28 m^2) is the
194 irradiated surface, V_T (80 L) is the total volume of the water into the pilot plant and Vi
195 (4.17 L) is the total irradiated volume. Each experiment was performed in duplicate and the
196 results were plotted as the average of the two replicates.

197

198 2.4 Selection of antibiotic resistant *E. coli* strain

199 The antibiotic resistant *E.coli* strain inoculated in GW for disinfection experiments was
200 isolated from the effluent of the biological process (activated sludge) of Almeria UWTP by
201 membrane filtration method and subsequent cultivation on selective medium, according to
202 a previously published procedure (Rizzo et al., 2014). More specifically, 50 mL of
203 wastewater and its serial dilutions were filtered through sterile membranes (cellulose
204 nitrate, 0.45-µm pore size, 47 mm diameter, Millipore) which were incubated (24 h, 37 °C)
205 on AR m-FC (Difco) culture medium supplemented with 64 mgL^{-1} of sulfamethoxazole.
206 Antibiotic concentration was chosen according to the double of the respective minimum
207 inhibitory concentration (MIC) values available in EUCAST database (2014). Some
208 colonies were randomly picked up and frozen at -5 °C using sterile vials of cryobeads
209 (Deltalab). To recover the stock, the vial was slowly unfreezed up to reach room
210 temperature (25 ºC). One bead was streaked onto a Petri dish of AR m-FC agar and

211 incubated for 20 h at 37 ºC to obtain isolated bacteria colonies. This dish was stored during
212 1 week in the refrigerator to prepare a fresh *E. coli* culture to make it available for GW
213 disinfection/oxidation experiments. Fresh liquid cultures were prepared taking one colony
214 from the refrigerated stock in the Petri dish using a loop, transferred into 14 mL of liquid
215 LB broth and incubated in a rotary shaker at 100 rpm, during 18-20 h at 37 ºC to get the
216 bacterial stationary phase concentration (10^9 CFU mL^{-1}). Bacterial suspensions were
217 harvested by centrifugation at 3000 rpm for 10 min. Then, the pellet was re-suspended in
218 Phosphate Buffer Saline (PBS) solution and diluted directly into the GW sample for each
219 experiment to reach the initial concentration of 10^6 CFUmL^{-1}.

220

221 2.5 Analytical measurements

222 Before performing each experiment, water samples were characterized in terms of
223 temperature, pH, conductivity, DOC, inorganic carbon (IC), total carbon (TC), anions and
224 cations. Temperature and pH were measured using a multi parametric sensor WTW
225 multi720. Conductivity was measured by a conductivity meter GLP31 CRISON. Turbidity
226 was measured by a turbidity meter 2100AN model (Hach). DOC, IC and TC were analyzed
227 using a Shimadzu TOC-V-CSN and an auto-sampler ASI-V. DOC was estimated as the
228 difference between the TC and the IC values. Samples were filtered with a 0.22 mm nylon
229 filter (Aisimo, Millipore Millex® GN) before their injection into the equipment. The
230 calibration was performed periodically with potassium hydrogen phthalate in Milli-Q water
231 for TC and a sodium carbonate/sodium bicarbonate (1:1) for IC. Anions and cations were
232 analyzed using ion chromatography, 850 Professional IC – Cation coupled to Metrohm 872
233 Extension Module. Samples were filtered with a 0.22 mm nylon filter (Aisimo) before
234 injection into the equipment. The calibration was checked before samples measurements
235 by standard solutions of 10 mg L^{-1} of each anion and cation analyzed. CECs concentrations

were monitored by ultra-performance liquid chromatography UPLC (Agilent Technologies, series 1200) with a UV-DAD detector and a C-18 analytical column. The initial conditions were 95% water with 25 mM formic acid (A) and 5% ACN (B). A linear gradient progressed from 10% to 0% B in 15 min. Re-equilibration time was 3 min with a flow rate of 1 $mL \cdot min^{-1}$. In order to prepare the vial for the detector, firstly, 4.5 mL of sample were filtered using a 0.22-µm PTFE filter (Millipore). Then, to remove any adsorbed compounds, the filter was washed with 2.5 mL of ACN mixed with the filtered water sample. The prepared solution was transferred into an amber glass vial, put in the UPLC and analyzed using an injection volume of 100 µL. Retention time, quantification limit (LOQ), detection limits (LOD) and maximum absorption (l) for the MCs are shown in Table S1 (in supplementary information file).

H_2O_2 concentration was measured with a spectrophotometer (PG Instruments Ltd T-60-U) at 410 nm in glass cuvettes with a 1 cm of path length based on the formation of a yellow complex from the reaction of titanium IV oxysulfate with H_2O_2 following DIN 38409 H15. Absorbance was read after 5 min incubation time against a H_2O_2 standard curve linear in the 0.1 - 100 mgL^{-1} concentration range.

PAA concentration was measured according to the method from HACH (2014). Briefly, 2.5 ml of sample was mixed with 15 mg of N,N-diethyl-p-phenylenediamine (DPD, VWR Chemicals). Absorbance was measured with a spectrophotometer (PG Instruments Ltd T-60-U) at 530 nm after 45 seconds of incubation time against a PAA standard curve (range 0.05 – 5 mg L^{-1}).

2.6 Bacterial count

Bacterial count was performed by standard plate counting method through a serial 10-fold dilutions in PBS placed into AR m-FC agar Petri dishes. In particular, when the bacterial load was expected to be high, 50 mL drop of adequate dilution was plated, instead, when the bacterial load was expected to be low, volume of 500 mL was spread onto prepared dishes. Antibiotic resistant (AR) *E.coli* colonies were counted after an incubation period of 20 h at 37 ºC (detection limit (DL) 2 $CFUmL^{-1}$). Measurements were carried out in duplicates in order to plot average values. The results were highly reproducible and the standard deviation of the replicates is showed in the graphs as error bars. Stock solutions of bovine liver catalase (50 mg L^{-1}) and sodium thiosulfate (100 mg L^{-1}) were freshly prepared every day and added 20 μL mL^{-1} and 1 μL mL^{-1} respectively to all water samples taken from the reactors in order to remove any residual concentration of PAA and H_2O_2.

3. Results

3.1 Inactivation of AR E. coli by sunlight/PAA in CPC

3.1.1 Control tests

Control experiments were performed with PAA and sunlight as standalone processes, respectively. The effect of PAA on the inactivation of AR *E. coli* under dark conditions was investigated for three PAA concentrations (0.075, 1 and 2 mg L^{-1}) in GW. The DL was achieved for 1 and 2 mg PAA L^{-1}, with 4 and 5 log unit inactivation respectively, after 15 min (Figure 1). The lower investigated dose (0.075 mg PAA L^{-1}) resulted only in half log unit inactivation after 180 min, possibly due to the low initial concentration of both PAA and H_2O_2 (0.039 mg L^{-1}). The DL was even achieved for sunlight experiment, but after 300 minutes treatment (53.67 kJL^{-1}).

Figure 1

Part of PAA initial concentration was consumed as the oxidant solution was added to GW sample; as can be observed from Figure SI1, PAA concentration measured just after the addition of PAA solution (t=0) is lower than the corresponding initial concentration dosed. Moreover, PAA was almost totally consumed after 300 min treatment when 1 mg PAA L^{-1} was added; while only 50% was consumed when initial PAA was 2 mg PAA L^{-1}.

3.1.2 Effect of PAA initial concentration

Since AR *E. coli* inactivation was quite fast between 1 and 2 mg PAA L^{-1} under dark conditions, lower PAA concentrations (in the range 0.075-1.0 mg L^{-1}) were investigated during sunlight/PAA tests. Q_{UV} and solar exposure time required to reach the DL for the inactivation of AR *E.coli*, decreased as PAA dose was increased. More specifically, in GW the best performance was achieved after 30 minutes with 0.2 mg PAA L^{-1} (Q_{UV} = 4.40 kJL^{-1}) (Figure 2a). Inactivation rates were faster compared to sunlight experiment where DL was achieved after 300 minutes treatment with a higher energy requirement (53.67 kJL^{-1}).

Figure 2

Moreover, the lower investigated PAA initial concentration (0.075 mg L^{-1}) did not produce a sufficient amount of hydroxyl radicals to improve AR *E.coli* inactivation compared to

304 solar radiation as standalone process. PAA was almost totally consumed during treatment
305 process (Figure SI2a) and a fluctuation in residual H_2O_2 concentration (1 mg PAA L^{-1}
306 solution) was observed (Figure SI2b).

307 The effect of sunlight/PAA process was also investigated in WW (Figure 2b). WW was not
308 inoculated with the selected AR *E. coli* strain, therefore the inactivation curves refer to the
309 indigenous *E. coli* population resistant to SMX (initial bacterial density 70-7000 CFU mL^{-1}
310). In particular, different initial PAA concentrations (1, 2, 4 and 10 mg L^{-1}) were
311 investigated and the best performance was observed for 10 mg PAA L^{-1} being the DL
312 achieved after 2 minutes irradiation (Q_{UV}= 0.28 kJL^{-1}) (Figure 2b). The DL was achieved
313 for all the investigated conditions, being the sunlight process the slower (Q_{UV}= 38.03 kJ L^{-1}
314 after 210 min). According to the results achieved in GW experiments, PAA was almost
315 totally consumed during treatment process in WW too and only when a higher dose (20 mg
316 L^{-1}) was investigated (to evaluate possible effect on CECs degradation) a residual was
317 detected (Figure SI3a). Fluctuation in residual H_2O_2 concentration (1 mg PAA L^{-1} solution)
318 was also observed in WW experiments (Figure SI3b).

319

320 *3.2 Degradation of CECs by sunlight/PAA in CPC*

321 Typically, when AOPs are investigated in the removal of pollutants from water, a matrix
322 effect can be observed, with a decreased process efficiency as the complexity of the
323 aqueous matrix increases (e.g., from deionized water solutions to GW and WW). The
324 decreased efficiency can be typically explained by the occurrence of easy to oxidize
325 molecules (also known as oxidant demand of the target water matrix) in more complex
326 water matrices compared to less complex ones. Actually, this behaviour was not evident in

the removal of CBZ and DCF by sunlight/PAA, while it was evident for SMX, as explained in the subsequent paragraphs.

3.2.1 Control tests

Control experiments to evaluate the effect of PAA and sunlight as standalone processes, on the target CECs were also carried out. In particular, the effect of PAA dose in darkness was investigated at 2 mg L^{-1} initial concentrations (Figure 3).

Figure 3

Unlike of CBZ, DCF was effectively oxidized by PAA after 60 minutes (80% removal), while SMX was removed at a lower rate (52% after 300 min) compared to DCF. Photodegradation rate by sunlight as standalone process changed depending on the target CEC: from no degradation for CBZ, to moderate degradation for SMX (43% after 300 min irradiation and 53.7 kJ L^{-1}), to high degradation for DCF (90% after 180 min and 30.2 kJ L^{-1}).

3.2.2 Effect of PAA initial concentration

The effect of sunlight/PAA process on CECs was investigated for both water matrices (GW and WW). CBZ was refractory to sunlight/PAA process too. Only when initial PAA concentration was increased to 10 mg L^{-1} a significant degradation (40%) was observed after 300 min treatment (Q_{UV} = 55.53 kJ L^{-1}) in GW (Figure 4a).

Figure 4

Even for DCF, sunlight/PAA process enhanced degradation compared to PAA as standalone process in GW matrix. The best performance was observed with 2 mg PAA L^{-1} that allowed to reach the quantification limit (QL) at Q_{UV} =10.23 kJ L^{-1} (Figure 4b). Interestingly, as PAA concentration was further increased from 4 to 10 mg L^{-1}, DCF degradation rate decreased. Similar behaviour was observed for SMX (Figure 4c). SMX degradation increased as PAA dose was increased from the lower dose (0.075 mg L^{-1}) to 4 mg L^{-1} (the QL was reached after 60 min and Q_{UV}= 9.49 kJ L^{-1}) then started to decrease, although to a lower rate compared to DCF.

Due to the higher oxidant demand of WW, PAA doses lower than 1.0 mg L^{-1} were not investigated and 20 mg PAA L^{-1} was added (Figure 5). The behaviour of sunlight/PAA process in WW matrix was quite different compared to GW. As matter of fact, a moderate efficiency in CBZ degradation was also observed at lower PAA doses; for example 2 mg PAA L^{-1} resulted in 23% CBZ degradation after 300 min (Q_{UV} = 58.39 kJ L^{-1}) and process efficiency increased as initial PAA concentration was increased to 4 and 10 mg L^{-1}, being the best removal (56%) observed with 10 mg PAA L^{-1} after 300 minutes (Q_{UV}= 58.39 kJ L^{-1}) (Figure 5a). But as PAA was further increased (20 mg L^{-1}), process efficiency drastically decreased, thus showing a similar behaviour to DCF and SMX in GW experiments.

Figure 5

372 DCF degradation was drastically affected by aqueous matrix. The best performance in
373 WW was observed with 20 mg PAA L^{-1} that reached the QL after 120 min (Q_{UV} = 11.46 kJ
374 L^{-1}) (Figure 5b). Moreover, aqueous matrix significantly affected process efficiency at
375 lower PAA concentrations; for example, only 32% degradation was achieved with 2 mgL^{-1}
376 of PAA in WW, compared to 99% observed in GW after 60 min treatment (Q_{UV} = 10.23 kJ
377 L^{-1}). Similarly to the results observed for GW, SMX degradation by sunlight/PAA
378 increased as PAA concentration was increased (Figure 5c). The QL was achieved for 10
379 mg L^{-1} of PAA after 240 min (Q_{UV}= 46.03 kJ L^{-1}). But a further increase of initial PAA
380 dose to 20 mg L^{-1} resulted in a decreased degradation efficiency, thus confirming the trend
381 already observed in GW experiments.

382

383 *3.3 Inactivation of AR E. coli by UV-C/PAA process*

384 Really fast inactivation rates were observed in GW for UV-C/PAA process compared to
385 sunlight/PAA (Figure 6). The detection limit was achieved for all PAA investigated doses
386 and even for UV-C as standalone process. In particular, total inactivation was achieved in a
387 few minutes for 0.15 mg PAA L^{-1} (2 min) and 0.2 mg PAA L^{-1} (4 min), but it is worthy to
388 mention that the initial AR *E. coli* concentrations were really low (47 and 240 CFU mL^{-1},
389 respectively).

390

391 **Figure 6**

392

393 With 0.075 mg L^{-1} and 0.1 mgL^{-1} of PAA DL was reached with a cumulative energy dose
394 of 67.39 kJL^{-1} (180 min irradiation) and 33.93 kJL^{-1} (90 min irradiation), respectively.

Due to both the higher oxidant demand of WW compared to GW and the total consumption of PAA and H_2O_2 in GW experiments, higher concentrations of PAA (4, 10 and 20 mgL^{-1}) were investigated in UV-C/PAA experiments in WW. Even in this case the initial AR *E. coli* concentrations were really low (63, 35 and 2 CFU mL^{-1} for 4, 10 and 20 mg PAA L^{-1} experiments, respectively) and the DL was achieved in 2 and 15 min for 10 and 4 mg PAA L^{-1} experiments, respectively (data not shown).

3.4 Degradation of CECs by UV-C/PAA process

The effect of PAA dose on the degradation of the target CECs by UV-C/PAA process was investigated in both water matrices (GW and WW). Among the three CECs, CBZ confirmed its lower degradation. No significant differences were observed between UV-C as standalone process (20% degradation after 180 minutes treatment and with an energy requirement of 71.78 kJ L^{-1}) and UV-C/PAA process up to 1.0 mg PAA L^{-1} in GW (Figure 7a). The best performance (77% removal) was obtained with 10 mg PAA L^{-1} after 150 minutes and with a Q_{UVC} of 71.78 kJ L^{-1}. Residual concentrations of PAA and H_2O_2 are available in supplementary information (Figures SI4a and SI4b).

Figure 7

For the lower concentration investigated in WW (4 mg PAA L^{-1}) the aqueous matrix effect between GW and WW was not observed (Figure 7b). But when PAA concentration was increased (10 and 20 mg PAA L^{-1}) the difference between the two matrices increased (e.g., 55% CBZ removal in WW compared to 67% in GW for 10 mg PAA L^{-1} at approximately

418 21 kJ L^{-1}). Interestingly, at the higher investigated dose (20 mg PAA L^{-1}), the residual
419 concentration of PAA is lower than that one for 10 mg PAA L^{-1} solution, but the
420 corresponding H_2O_2 residual concentration is significantly higher (Figure SI5).

421 The best degradation of DCF in GW was already observed for the lower investigated PAA
422 doses (0.075 mg PAA L^{-1}) compared to sunlight/PAA tests (Figure 8a). Even in UV-
423 C/PAA tests, process efficiency started to decrease above a certain concentration (1.0 mg
424 L^{-1}) of PAA, being the worst removal observed for the higher investigated PAA dose (10
425 mg L^{-1}). The water matrix affected the photo-oxidation process, because no drastic
426 efficiency decrease was observed as PAA was increased (Figure 8b).

427

428 **Figure 8**

429

430 SMX was effectively degraded even with UV-C as stand-alone process in GW (DL was
431 achieved with Q_{UV}= 5.78 kJ L^{-1}) and WW (DL observed for $Q_{UV<}$ 4.58 kJ L^{-1}), accordingly
432 PAA addition did not significantly improve process efficiency (for 4 mg PAA L^{-1} DL
433 observed for $Q_{UV<}$ 2.4 kJ L^{-1}) (data not shown).

434

435 **4. Discussion**

436 *4.1 Photolysis of PAA and effect on PAA and H_2O_2 concentrations*

437 UV/PAA process has been poorly investigated so far, and the previous works have been
438 basically focused on bacteria inactivation (Koivunen and Heinonen-Tanski, 2005; de
439 Souza et al. 2015); only recently its effect on pharmaceuticals has been addressed (Cai et

al., 2017). PAA (CH_3CO_3H) aqueous solutions commercially available are an equilibrium mixture of acetic acid (CH_3COOH), H_2O_2, PAA and water, according to the reaction:

$$CH_3COOH + H_2O_2 \leftrightarrow CH_3CO_3H + H_2O \quad \text{(Eq.3)}$$

Photolysis of the O–O bond in the PAA molecule results in the formation of $HO^{\bullet}$, according to Equation 4 (Caretti and Lubello, 2003):

$$CH_3CO_3H + hv \rightarrow CH_3COO^{\bullet} + HO^{\bullet} \quad \text{(Eq.4)}$$

The $CH_3COO^{\bullet}$ molecule will rapidly split in $CH_3^{\bullet}$ and CO_2 (Martin and Gehr, 2007). Moreover, $HO^{\bullet}$ molecules can also recombine to form H_2O_2:

$$HO^{\bullet} + HO^{\bullet} \rightarrow H_2O_2 \quad \text{(Eq.5)}$$

The production of PAA (Eq.3) and the recombination of $HO^{\bullet}$ molecules (Eq.5) can explain the fluctuations observed in the measurement of residual H_2O_2 (Figure SI2b and SI3b).

According to the results achieved in this work, the mechanisms of bacterial inactivation and CECs degradation in PAA photolysis are possible related to a combination of effects including photolysis, oxidation (by PAA solution) and formation of $HO^{\bullet}$.

4.2 Control tests: effect of radiation and PAA solution on bacteria inactivation and CECs degradation

The effect of sunlight and UV-C radiation on bacteria inactivation is evident from figures 2 and 6, respectively. To date, all waterborne pathogenic bacteria, among which *E. coli*, have been found to be amenable to sunlight disinfection (McGuigan et al., 2012). Although the UV-A wavelengths are not sufficiently energetic to alter DNA directly, UV-A play an important role in promoting the formation of intracellular reactive oxygen species (e.g.,

462 $HO^{\bullet}$) which can, in turn, damage DNA. UV-C radiation (200–280 nm germicidal
463 wavelength range, peaks at about 260–265 nm) has a direct effect on bacterial cells
464 because it is absorbed by nucleic acids; cell inactivation can take place through UV-
465 induced damages such as the formation of pyrimidine dimers in their DNA (Kowalski,
466 2009).

467 While CBZ was not (under sunlight in GW) or poorly (under sunlight in WW and under
468 UV-C radiation) photodegraded, confirming its refractory behaviour to direct photolysis
469 (Calisto et al., 2011), SMX and DCF were significantly degraded under irradiation. DCF
470 has an absorbance peak at 275-280 nm and its degradation under sunlight is the result of
471 two mechanisms: direct photolysis and self-sensitization, being direct photolysis the main
472 one (Zhang et al., 2011). SMX absorbance spectrum is characterized by a peak at 257-268
473 nm (depending on solution pH) and tails well over 320 nm, which overlap to solar
474 spectrum (in the 300–325 nm) and make its photodegradation possible (Trovò et al., 2009;
475 Rizzo et al., 2012).

476 The redox potential of PAA is comparable or even higher than many disinfectants (Zhang
477 et al., 2018), which make it effective in the inactivation of different bacterial populations.
478 Accordingly, our results in terms of AR *E. coli* inactivation under dark conditions (Figure
479 1) are consistent with previous results on *E. coli* inactivation (Antonelli et al., 2009).
480 Moreover, the high redox potential can also explain the high oxidation rate of DCF and
481 SMX (Figure 3).

482

4.3 Effect of photo driven AOPs with PAA on bacteria inactivation and CECs degradation

According to Eq.4, sunlight/PAA and UV-C/PAA processes result in the formation of $HO^{\bullet}$ species. The role of $HO^{\bullet}$ in the inactivation of *E. coli* was previously explained through the support of disinfection photocatalytic experiments (Cho et al. 2004). In subsequent studies, a killing mechanism where $HO^{\bullet}$ progressively damages the cell surface structures leading to the release of intracellular material/molecules was proposed (Foster et al., 2011). Inactivation of microorganisms by photo driven advanced oxidation with PAA has been mainly investigated by using artificial light while, to our knowledge, only one study was specifically focused on sunlight/PAA process (Formisano et al., 2016) and no previous study evaluated the effect on the inactivation of AR *E. coli*. Formisano et al. (2016) observed a total inactivation of *E. coli* by sunlight/PAA (8 mg PAA L^{-1}) process after 120 minutes treatment (Q_{UV}= 7.42 kJ L^{-1}) in WW, with an initial *E. coli* density as high as 10^5 CFU mL^{-1}. These results are different compared to the inactivation rates observed in our work with (i) GW (where the best performance was achieved after 30 minutes with 0.2 mg PAA L^{-1} and Q_{UV} = 4.40 kJ L^{-1}) (Figure 2a) and (ii) WW (being the best performance and DL achieved for 10 mg PAA L^{-1} after 2 minutes irradiation and Q_{UV}= 0.28 kJ L^{-1}) (Figure 2b). The different water matrix and *E. coli* population (total Vs AR *E. coli*) in case (i) and the lower initial bacterial density and the different *E. coli* population in case (ii) may explain the different results observed. Inactivation rates in GW drastically increased when UV-C radiation was used (DL achieved within 2 minutes for 0.15 mg PAA L^{-1} and 4 minutes with 0.2 mg PAA L^{-1}) instead of sunlight. In WW experiments, the initial AR *E. coli* concentration was really low and the DL was achieved for all the PAA doses investigated. In a previous work on wastewater disinfection by UV-C/PAA process, *E. coli*

507 inactivation of 3.6 and 4.5 log units were observed for 2 and 4 mg L^{-1} of PAA, respectively
508 and an UV-C dose as high as UV dose of 120 mW·s cm^{-2} (Lubello et al., 2002).

509 As the effect of photo driven AOPs with PAA on CECs degradation is of concern, it is
510 worthy to mention that scientific literature is lacking. However, our results are consistent
511 with removal trends of CBZ, DCF and SMX observed in solar driven AOPs (namely
512 photo-Fenton) (Klamerth et al., 2010; Ferro et al., 2015). In our work CBZ was found to be
513 refractory to sunlight/PAA process, according to the results available in the literature for
514 other solar driven AOPs. For example, only 36.9% degradation (same initial CBZ
515 concentration) was observed after 300 minute sunlight/H_2O_2 (20 mg L^{-1}) treatment
516 (Q_{UV}=19.3 kJ L^{-1}) in WW (Ferro et al., 2015). When UV-C radiation was used as light
517 source in UV-C/PAA process, an higher efficiency was observed (77% removal,
518 Q_{UV}=71,78 kJ L^{-1}), but the removal efficiency (22%) observed for 1 mg PAA L^{-1} is not
519 consistent with previous work (90% removal within 30 min, CBZ initial concentration 1
520 μM) (Cai et al., 2017). Unlike of CBZ, high removal efficiencies were observed for DCF
521 and SMX in sunlight/PAA experiments, with significantly improved removals in UV-
522 C/PAA tests. However, DCF degradation was drastically affected by aqueous matrix, with
523 a remarkable decreased efficiency in WW (Figure 5b) compared to GW (Figure 4b), in
524 particular at lower PAA concentrations. These results can be explained by the higher
525 oxidant demand of WW compared to GW (confirmed by the PAA and H_2O_2 consumption
526 for tests with low concentrations of PAA, Figures SI2 and SI3). Matrix effect was also
527 observed for SMX degradation by sunlight/PAA and its removal is consistent with
528 previous works with other solar driven AOPs. As matter of fact, Karaolia et al. (2017)
529 observed complete removal of SMX (initial spiked concentration 100 μg L^{-1}) by solar
530 photo-Fenton in urban wastewater in a CPC reactor (50 mg H_2O_2 L^{-1} and 5 mg Fe^{2+} L^{-1},
531 119 min of normalized irradiation time ($t_{30W,n}$)).

532 Interestingly, similar removal trends were observed for DCF and SMX in sunlight/PAA
533 experiments, in both water matrices investigated. The removal efficiency first increased as
534 initial PAA was increased, then started to decrease. Possibly, the reduced efficiency may
535 be due to the scavenging effect of PAA on $HO^{\bullet}$ because of the higher PAA concentration
536 (Cai et al., 2017).

537

538 **5. Conclusions**

539 Photo driven AOP with PAA was investigated as possible tertiary treatment method of
540 urban wastewater by evaluating its efficiency in the inactivation of AR *E. coli* and
541 degradation of a mixture of three CECs under different light sources. Low PAA doses were
542 found to be effective in the inactivation of AR *E. coli*, being UV-C driven process faster
543 (DL achieved at Q_{UV}=0.3 kJ L^{-1} with 0.2 mg PAA L^{-1}) than solar driven one (DL achieved
544 at Q_{UV}=4.4 kJ L^{-1} with 0.2 mg PAA L^{-1}). Higher Q_{UV} and PAA initial doses are necessary
545 to effectively remove the target CECs (being CBZ the more refractory) and, although
546 process efficiency in sunlight tests is lower compared to UV-C radiation, sunlight driven
547 process is still an interesting option for small wastewater treatment plants taking into
548 account that CECs occur at low concentrations (typically in the range ng L^{-1} - fractions of
549 μg L^{-1}). However, initial PAA dose should be optimized to find the best compromise
550 between target bacteria inactivation and CECs removal as well as to prevent scavenging
551 effect of PAA on $HO^{\bullet}$ because of high PAA concentration.

552

553 **Acknowledgements**

554 The authors wish to thank European Commission for supporting Teresa Agovino's visit at
555 Plataforma Solar de Almeria in the context of ERASMUS programme.

556

557 **References**

558 Ahmed, M. J., 2017. Adsorption of quinolone, tetracycline, and penicillin antibiotics from
559 aqueous solution using activated carbons: Review. Environmental Toxicology and
560 Pharmacology 50, 1-10.

561 Antonelli, M., Rossi, S., Mezzanotte, V., Nurizzo, C. 2006. Secondary Effluent
562 Disinfection: PAA Long Term Efficiency. Environmental Science & Technology 40, 4771-
563 4775.

564 Antonelli, M., Turolla, A., Mezzanotte, V., Nurizzo, C. 2013. Peracetic acid for secondary
565 effluent disinfection: A comprehensive performance assessment. Water Science &
566 Technology 68 (12), 2638-2644.

567 Bourgin, M., Beck, B., Boehler, M., Borowska, E., Fleiner, J., Salhi, E., Teichler, R., von
568 Gunten, U., Siegrist, H., McArdell, C. S., 2018. Evaluation of a full-scale wastewater
569 treatment plant upgraded with ozonation and biological post-treatments: Abatement of
570 micropollutants, formation of transformation products and oxidation by-products. Water
571 Research 129, 486-498.

572 Brack, W., Dulio, V., Ågerstrand, M., Allan, I., Altenburger, R., Brinkmann, M., Bunke,
573 D., Burgess, R.M., Cousins, I., Escher, B.I., Hernández, F.J., Hewitt, L.M., Hilscherová,
574 K., Hollender, J., Hollert, H., Kase, R., Klauer, B., Lindim, C., López Herráez, D., Miège,
575 C., Munthe, J., O'Toole, S., Posthuma, L., Rüdel, H., Schäfer, R.B., Sengl, M., Smedes, F.,
576 van de Meent, D., van den Brink, P.J., van Gils, J., van Wezel, A.P., Vethaak, A.D.,
577 Vermeirssen, E., von der Ohe, P.C., Vrana, B. 2017. Towards the review of the European
578 Union Water Framework management of chemical contamination in European surface
579 water resources. Science of the Total Environment 576, 720–737.

580 Cai, M., Sun, P., Zhang, L., Huang, C.-H. 2017. UV/Peracetic Acid for Degradation of
581 Pharmaceuticals and Reactive Species Evaluation. Environmental Science & Technology
582 51, 14217-14224.

583 Calisto, V., Rosário Domingues, M., Erny, G.L., Esteves, V.I. 2011. Direct
584 photodegradation of carbamazepine followed by micellar electrokinetic chromatography
585 and mass spectrometry. Water Research 45, 1095-1104.

586 Caretti, C., Lubello, C. 2003. Wastewater disinfection with PAA and UV combined
587 treatment: a pilot plant study. Water Research 37, 2365-2371.

588 Cho, M., Chung, H., Choi, W., Yoon, J. 2004. Linear correlation between inactivation of
589 E. coli and OH radical concentration in TiO2 photocatalytic disinfection. Water Research
590 38, 1069-1077.

591 De Souza, J.B., Queiroz Valdez, F., Jeranoski, R.F., de Sousa Vidal, C.M., Soares
592 Cavallini, G. 2015. Water and Wastewater Disinfection with Peracetic Acid and UV
593 Radiation and Using Advanced Oxidative Process PAA/UV. International Journal of
594 Photoenergy, Article ID 860845, http://dx.doi.org/10.1155/2015/860845

595 Fatta-Kassinos, D., Manaia, C., Berendonk, T.U., Cytryn, E., Bayona, J., Chefetz, B.,
596 Slobodnik, J., Kreuzinger, N., Rizzo, L., Malato, S., Lundy, L., Ledin, A. COST Action
597 ES1403: New and Emerging challenges and opportunities in wastewater REUSe
598 (NEREUS). Environmental Science Pollution Research 22, 7183-7186.

599 Ferro, G., Polo-López, M.I., Martínez-Piernas, A.B., Fernández-Ibáñez, P., Agüera A.,
600 Rizzo L. 2015. Cross-Contamination of Residual Emerging Contaminants and Antibiotic
601 Resistant Bacteria in Lettuce Crops and Soil Irrigated with Wastewater Treated by
602 sunlight/H_2O_2. Environmental Science & Technology 49, 11096-11104.

603 Fiorentino, A., Ferro, G., Castro, A.M., Polo-López, M.I., Fernández-Ibañez, P., Rizzo, L.
604 2015. Inactivation and regrowth of multidrug resistant bacteria in urban wastewater after
605 disinfection by solar-driven and chlorination processes. Journal of Photochemistry and
606 Photobiology B: Biology 148, 43-50.

607 Formisano, F., Fiorentino, A., Rizzo, L., Carotenuto, M., Pucci, L., Giugni, M., Lofrano,
608 G. 2016. Inactivation of Escherichia coli and Enterococci in urban wastewater by
609 sunlight/PAA and sunlight/H2O2 processes. Process Safety and Environmental Protection
610 104, 178-184.

611 Foster, H.A., Ditta, I.B., Varghese, S., Steele, A. 2011. Photocatalytic disinfection using
612 titanium dioxide: spectrum and mechanism of antimicrobial activity. Applied
613 Microbiology Biotechnology 90, 1847-1868.

614 Fu, W., Li, B., Yan, J., Y, H., Liyuan, C., Li, X. 2018. New insights into the chlorination of
615 sulfonamide: Smiles-type rearrangement, desulfation, and product toxicity. Chemical
616 Engineering Journal 331, 785-793.

617 HACH, 2014. Determination of Peracetic Acid and Hydrogen Peroxide in Water.
618 Application Note.

619 Hollender, J., Zimmermann, S.G., Koepke, S., Krauss, M., Mcardell, C.S., Ort, C., Singer,
620 H., von Gunten, U., Hansruedi, S. 2009. Elimination of Organic Micropollutants in a
621 Municipal Wastewater Treatment Plant Upgraded with a Full-Scale Post-Ozonation
622 Followed by Sand Filtration. Environmental Science & Technology 43, 7862-7869.

623 Huang, H., Wu, Q.-Y., Tang, X., Jiang, R., Hu, H.-Y. 2016. Formation of haloacetonitriles
624 and haloacetamides and their precursors during chlorination of secondary effluents.
625 Chemosphere 144, 297-303.

626 ISO 16075 (2015). Guidelines for Treated Wastewater Use for Irrigation Projects.
627 International Organization for Standardization, Geneva, Switzerland.

628 JRC (Joint Research Centre), 2015. Development of the first Watch List under the
629 Environmental Quality Standards Directive: Directive 2008/105/EC, as amended by
630 Directive 2013/39/EU, in the field of water policy. Raquel N. Carvalho, Lidia Ceriani,
631 Alessio Ippolito and Teresa Lettieri. Report EUR 27142 EN.

632 Karaolia, P., Michael-Kordatou, I., Hapeshi, E., Alexander, J., Schwartz, T., Fatta-
633 Kassinos, D. 2017. Investigation of the potential of a Membrane BioReactor followed by
634 solar Fenton oxidation to remove antibiotic-related microcontaminants. Chemical
635 Engineering Journal 310, 491-502.

636 Keun-Young, P., Su-Young C., Seung-Hoon L., Ji-Hyang K., Ji-Hyeon S. 2016.
637 Comparison of formation of disinfection by-products by chlorination and ozonation of
638 wastewater effluents and their toxicity to Daphnia magna. Environmental Pollution 215,
639 314-321.

640 Klamerth, N., Rizzo, L., Malato, S., Maldonado, M.I., Agüera, A., Fernández-Alba, A.R.
641 2010. Degradation of fifteen emerging contaminants at μg L-1 initial concentrations by
642 mild solar photo-Fenton in MWTP effluents. Water Research 44, 545-554.

643 Koivunen, J., Heinonen-Tanski, H. 2005. Inactivation of enteric microorganisms with
644 chemical disinfectants, UV irradiation and combined chemical/UV treatments. Water
645 Research 39, 1519-1526.

646 Kowalski, W. 2009. Ultraviolet Germicidal Irradiation Handbook, DOI 10.1007/978-3-
647 642-01999-9_2, Springer-Verlag Berlin Heidelberg.

Krzeminski, P., Tomei, M.C., Karaolia, P., Langenhoff, A., Almeida, C.M.A., Felis, E., Gritten, F., Andersen, H.R., Fernandes T., Manaia, C.M., Rizzo, L., Fatta-Kassinos, D. 2019. Performance of secondary wastewater treatment methods for the removal of contaminants of emerging concern implicated in crop uptake and antibiotic resistance spread: A review. Science of the Total Environment 648, 1052-1081.

Lian, J., Qiang, Z., Li, M., Bolton, J.R., Qu, J. 2015. UV photolysis kinetics of sulfonamides in aqueous solution based on optimized fluence quantification. Water Research 75, 43-50.

Lubello, C., Caretti, C., Gori, R., 2002. Comparison between PAA/UV and H2O2/UV disinfection for wastewater reuse. Water Science and Technology.: Water Supply 2(1), 205-212.

Malato, S., Fernandez-Ibanez, P., Maldonado, M.I., Blanco, J., Gernjak, W., 2009. Decontamination and disinfection of water by solar photocatalysis: recent overview and trends. Catalysis Today 147, 1–59.

Martin, N., Gehr, R., 2007. Reduction of Photoreactivation with the Combined UV/Peracetic Acid Process or by Delayed Exposure to Visible Light. Water Environment Research 79, 991-999.

McGuigan, K.G., Conroy, R.M., Mosler, H.-J., du Preez, M., Ubomba-Jaswa, E., Fernandez-Ibanez, P. 2012. Solar water disinfection (SODIS): a review from bench-top to roof-top. Journal of Hazardous Materials 235-236, 29-46.

Petrie, B., Barden, R., Kasprzyk-Hordern B. 2015. A review on emerging contaminants in wastewaters and the environment: Current knowledge, understudied areas and recommendations for future monitoring. Water Research 72, 3-27.

671 Polo-López, M.I., Fernández-Ibáñez, P., García-Fernández, I., Oller, I., Salgado-Tránsito,
672 I., Sichel, C. 2010. Resistance of Fusarium sp spores to solar TiO_2 photocatalysis:
673 influence of spore type and water (scaling-up results). Journal of Chemical Technology
674 and Biotechnology 85, 1038–1048.

675 Rizzo, L., Della Sala, A., Fiorentino, A., Li Puma, G. 2014. Disinfection of urban
676 wastewater by solar driven and UV lamp – TiO2 photocatalysis: effect on a multi drug
677 resistant Escherichia coli strain, Water Research 53, 145-152.

678 Rizzo, L., Fiorentino, A., Anselmo, A. 2012. Effect of solar radiation on multidrug
679 resistant E. coli strains and antibiotic mixture photodegradation in wastewater polluted
680 stream. Science of the Total Environment 427-428, 263-268.

681 Rizzo, L., Fiorentino, A., Grassi, M, Attanasio, D., Guida M. 2015. Advanced treatment of
682 urban wastewater by sand filtration and graphene adsorption for wastewater reuse: Effect
683 on a mixture of pharmaceuticals and toxicity. Journal of Environmental Chemical
684 Engineering 3, 122-128.

685 Rizzo, L., Kraetke, R., Linders, J., Scott, M., Vighi, M., de Voogt, P. 2018. Proposed EU
686 minimum quality requirements for water reuse in agricultural irrigation and aquifer
687 recharge: SCHEER scientific advice. Current Opinion in Environmental Science & Health
688 2, 7–11.

689 Rizzo, L., Manaia, C.M., Merlin, C., Schwartz, T., Dagot, C., Ploy, M.C., Michael, I.,
690 Fatta-Kassinos, D., 2013. Urban wastewater treatment plants as hotspots for antibiotic
691 resistant bacteria and genes spread into the environment: a review. Science of the Total
692 Environment 447, 345–360.

693 Sacco, O., Vaiano, V., Rizzo, L., Sannino, D. 2018. Photocatalytic activity of a visible
694 light active structured photocatalyst developed for municipal wastewater treatment. Journal
695 of Cleaner Production 175, 38-49.

696 Trovó, A.G., Nogueira, R.F.P., Agüera, A., Sirtori, C., Fernández-Alba, A.R. 2009.
697 Photodegradation of sulfamethoxazole in various aqueous media: Persistence, toxicity and
698 photoproducts assessment. Chemosphere 77, 1292-1298.

699 USEPA. 2012. Guidelines for water reuse. (EPA/600/R-12/618) United States
700 Environmental Protection Agency, Washington, DC, USA.

701 Yuan, Q., Guo, M., Yang, J. 2015. Fate of antibiotic resistant bacteria and genes during
702 wastewater chlorination: implication for antibiotic resistance control. PloS One 10 (3),
703 e0119403.

704 Zhang, C., Brown, P.J.B., Hu, Z. 2018. Thermodynamic properties of an emerging
705 chemical disinfectant, peracetic acid. Science of the Total Environment 621, 948-959.

706 Zhang, N., Liu, G, Liu, H., Wang, Y., He, Z., Wang, G. 2011. Diclofenac
707 photodegradation under simulated sunlight: Effect of different forms of nitrogen and
708 Kinetics. Journal of Hazardous Materials 192, 411-418.

709 Figure captions

710 Figure 1. Inactivation of AR *E. coli*: control tests in dark with PAA and sunlight as
711 standalone processes. Q_{UV} values are given between brackets.

712 Figure 2. Inactivation of AR *E. coli* by sunlight/PAA in CPC: effect of initial PAA
713 concentration.

714 Figure 3. Degradation of CECs: control tests with PAA and sunlight as standalone
715 processes.

716 Figure 4. Effect of sunlight/PAA process on CECs in GW: CBZ (a), DCF (b) and SMX (c).

717 Figure 5. Effect of sunlight/PAA process on CECs in WW: CBZ (a), DCF (b) and SMX
718 (c).

719 Figure 6. Inactivation of AR *E. coli* by UV-C/PAA process.

720 Figure 7. Effect of UV-C/PAA process on CBZ in GW (a) and WW (b).

721 Figure 8. Effect of UV-C/PAA process on DCF in GW (a) and WW (b).

Table 1: physical-chemical characteristics of GW and WW samples.

	GW	WW
Parameters	**Av ± SD**	**Av ± SD**
Cl^- (mg L^{-1})	337.1 ± 76.7	341.3 ± 16.3
NO_3^- (mg L^{-1})	12.1 ± 1.2	23.4 ± 5.3
SO_4^{2-} (mg L^{-1})	200.9 ± 39.6	84.3 ± 7.7
NH_4^+ (mg L^{-1})	-	23.6 ± 24.2
Na^+ (mg L^{-1})	517.8 ± 94.1	197.5±2.8
Mg^{2+} (mg L^{-1})	67.2 ± 15.4	31.4 ± 6.9
K^+ (mg L^{-1})	8.87 ± 1.7	27.1 ± 0.8
Ca^{2+} (mg L^{-1})	71.6 ± 16.8	71.4 ± 11.8
pH	8.2 ± 0.5	7.5 ± 0.1
Conductividad (μS cm^{-1})	2396.0 ± 0.10	1921.0 ± 21.4
Turbidez (NTU)	0.6 ± 0.1	6.3 ± 4.4
TOC (mg L^{-1})	1.80 ± 1.6	24 ± 1.0
IC (mg L^{-1})	170.2 ± 9.3	38 ± 8.1

Figure1

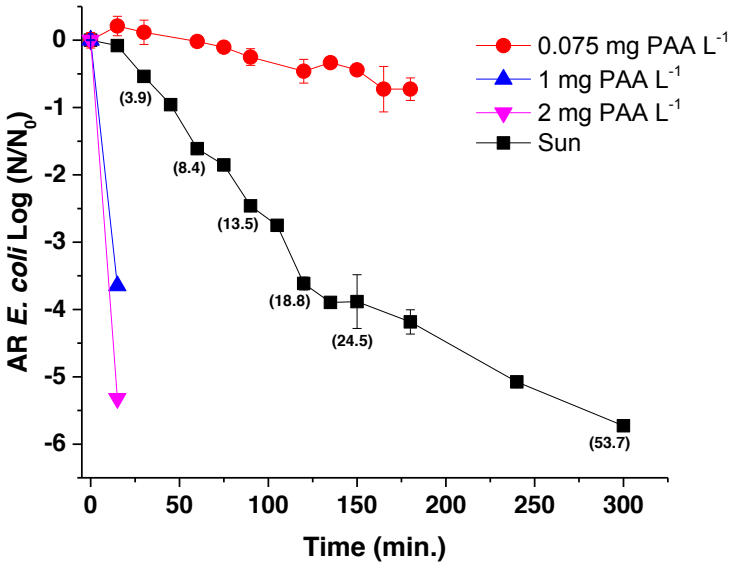

Figure 1

Figure2

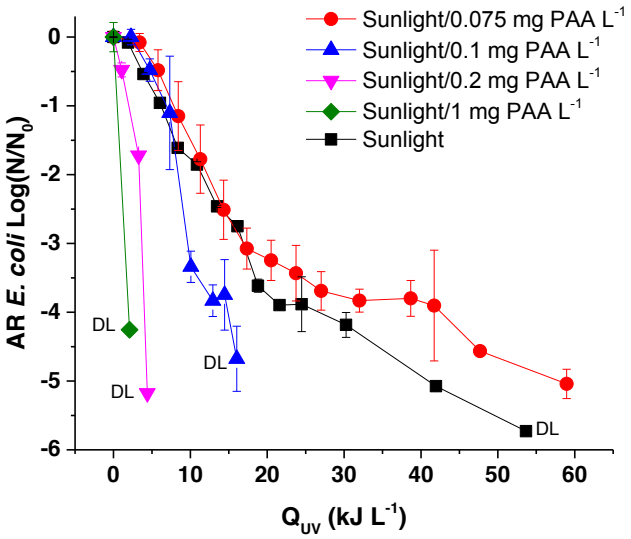

a)

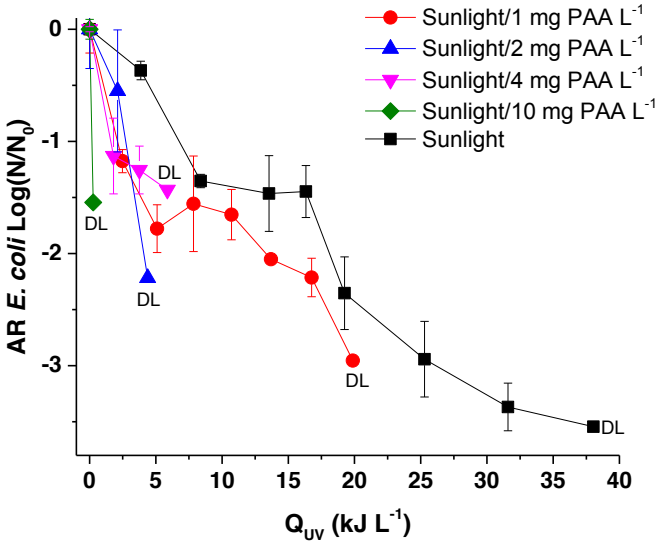

b)

Figure 2

Figure3

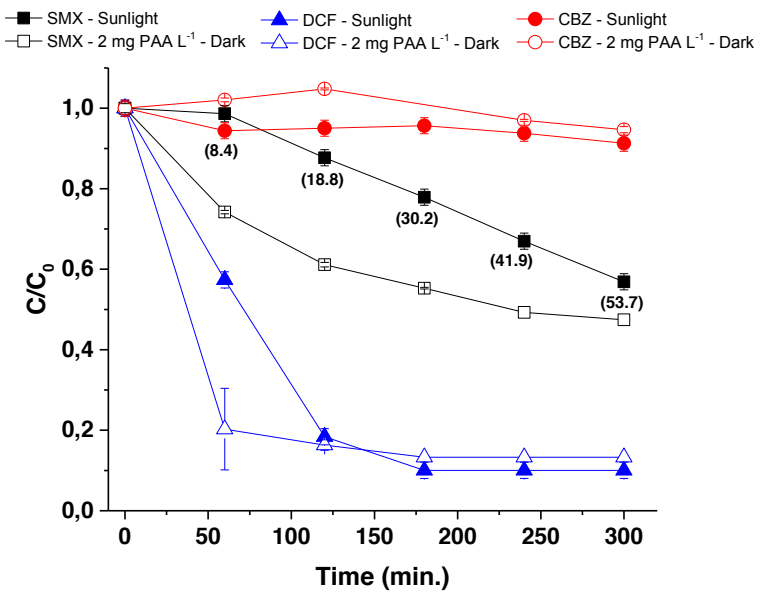

Figure 3

Figure4

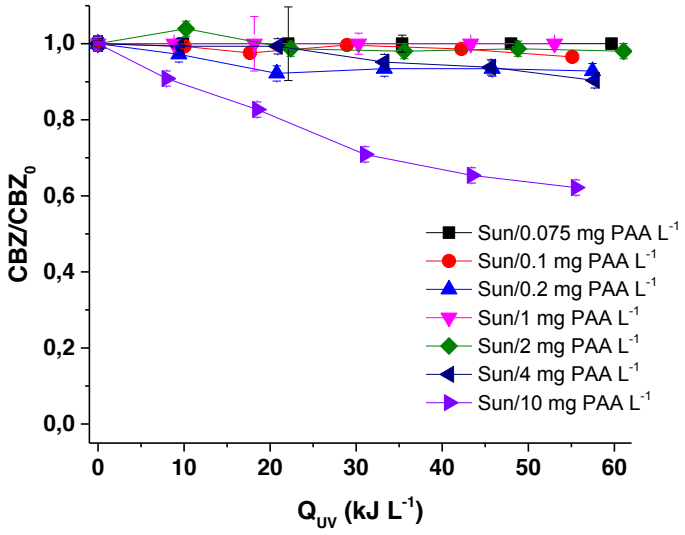

a)

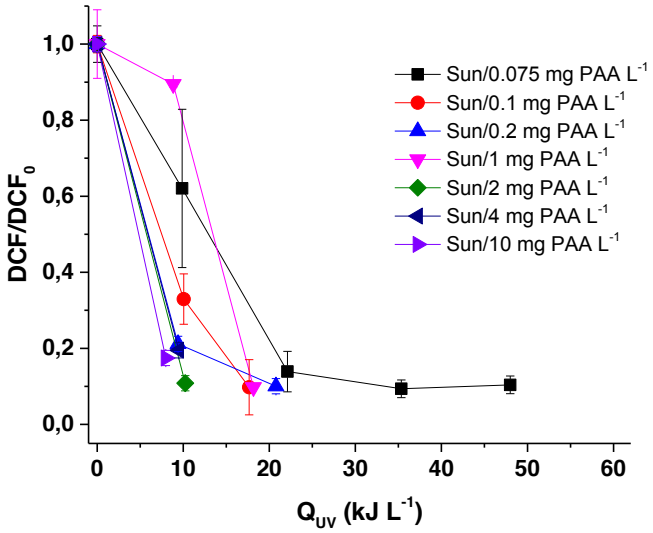

b)

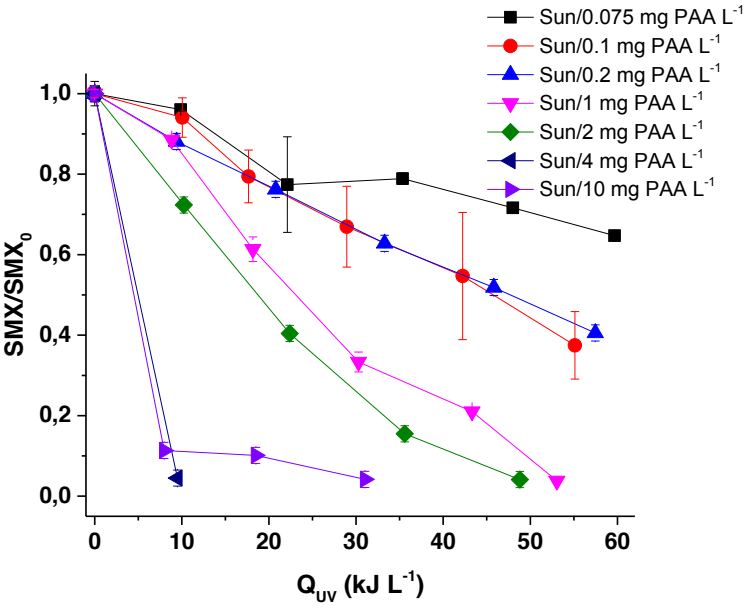

c)

Figure 4

Figure5

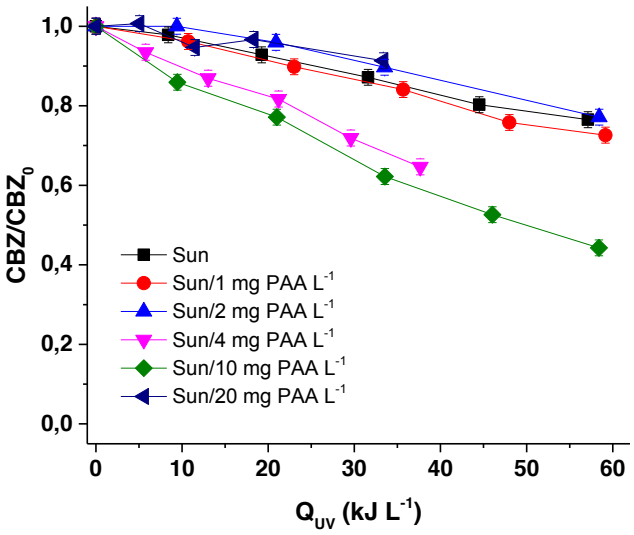

a)

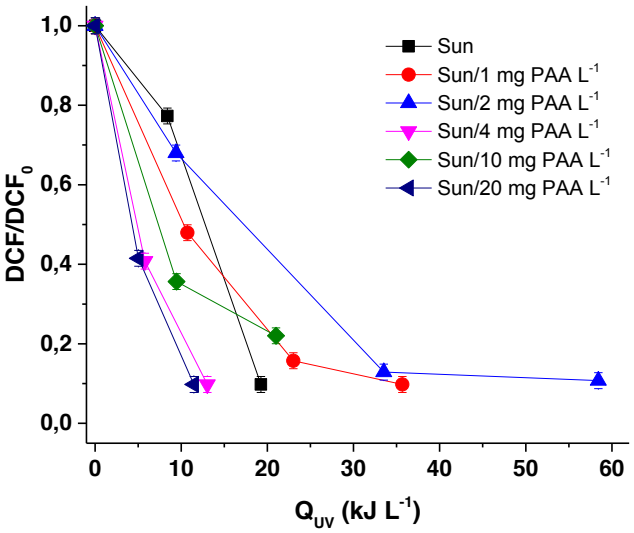

b)

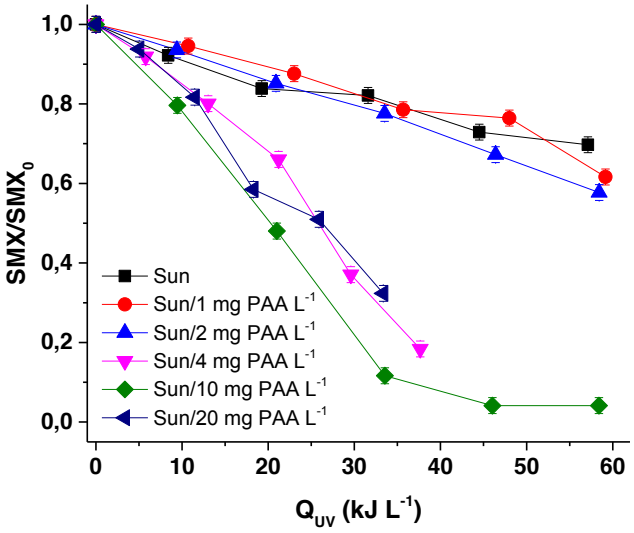

c)

Figure 5

Figure6

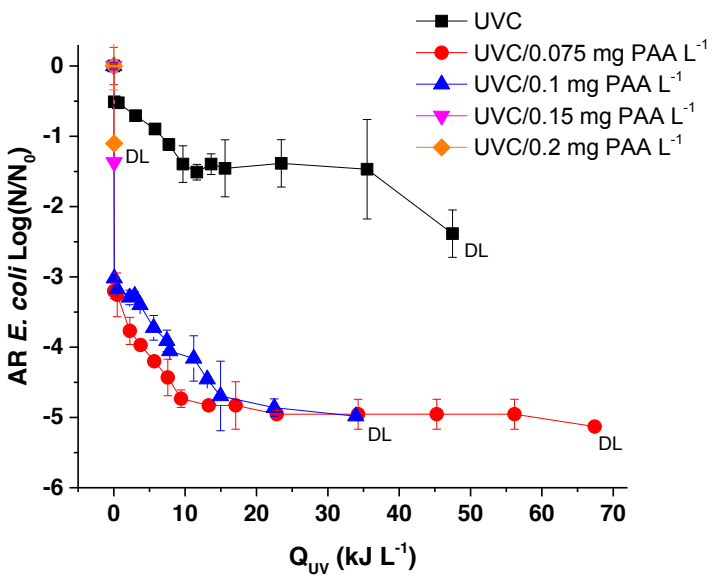

Figure 6

Figure7

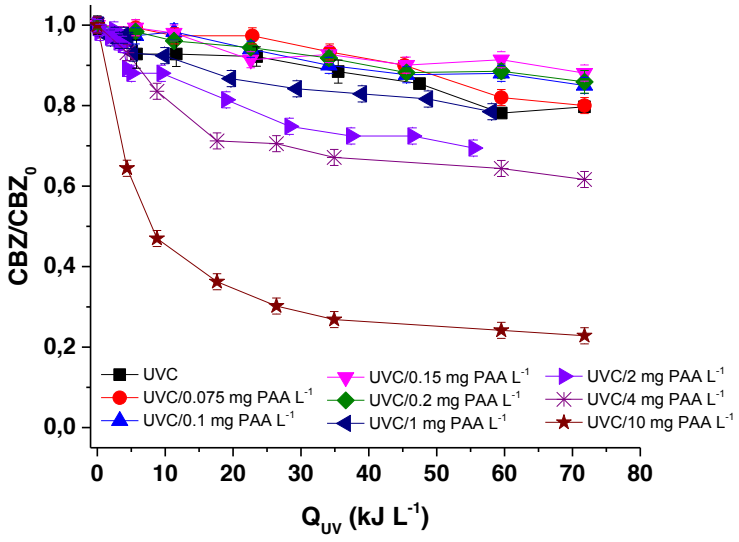

a)

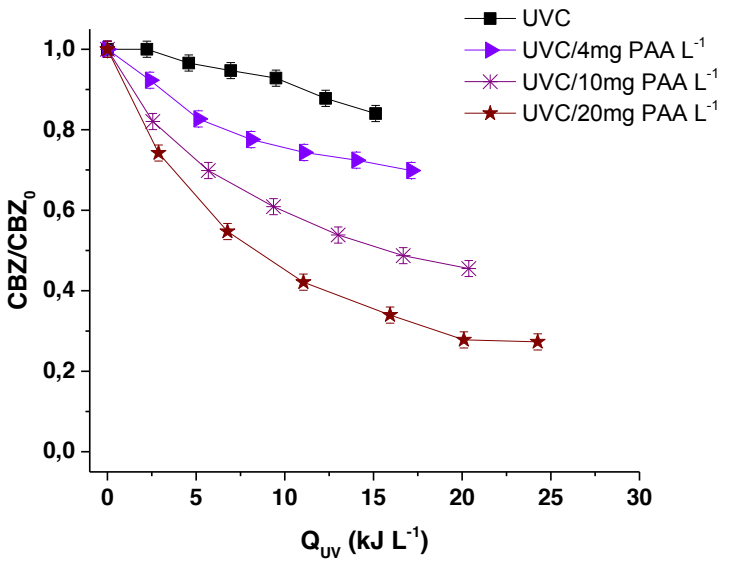

b)

Figure 7

Figure8

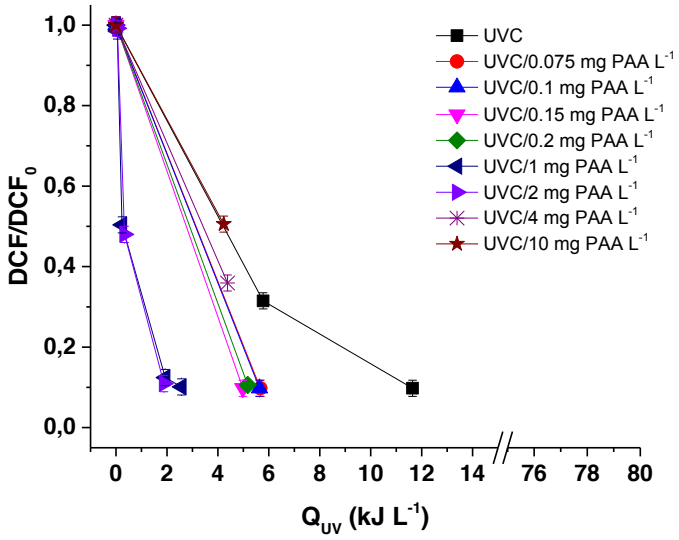

a)

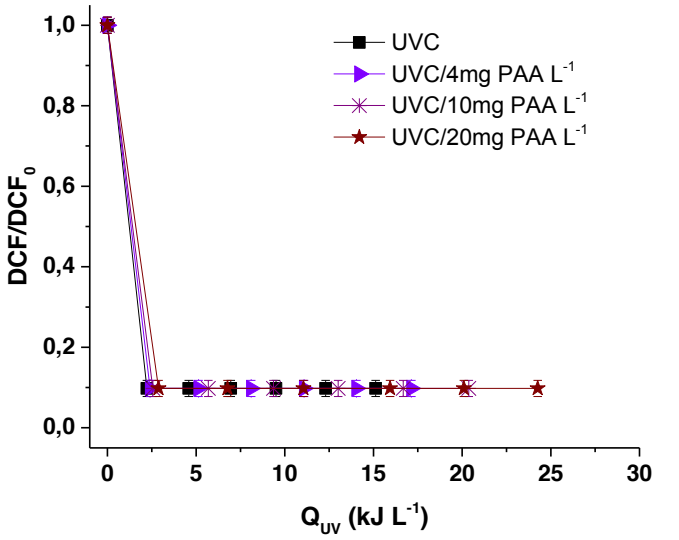

b)

Figure 8

Electronic Supplementary Material (for online publication only)

Click here to download Electronic Supplementary Material (for online publication only): Supplementary information.docx